Upper Limits on Achievable Storage Density Using Turbo Equalization in 2-D Magnetic Recording

Jaehyeong No and Jaekyun Moon, *Fellow, IEEE*

Department of Electrical Engineering, Korea Advanced Institute of Science and Technology, Daejeon 305-701, Korea

The maximum amounts of 2-D intersymbol interference that can be tolerated by the specific types of turbo equalizers are analyzed using the extrinsic information transfer charts. The results translate into the maximum normalized user density that each equalizer can support given an ample channel signal-to-noise ratio. It is shown that a low-complexity self-iterating equalizer based on individually weak linear component equalizers running in different directions provides excellent performance.

***Index Terms*— 2-D intersymbol interference (ISI), extrinsic information transfer (EXIT) chart, soft-in soft-out (SISO) linear equalizer (LE), turbo equalizer.**

I. Introduction

INTERSYMBOL interference (ISI) in 2-D magnetic recording presents a serious issue in the reliable recovery of stored data. Powerful modern equalization methods are based on the turbo equalization principle wherein a soft-in soft-out (SISO) equalizer and a SISO error correction decoder exchange soft information in an iterative fashion until the effect of interference is suppressed. Trellis-based equalizers, like the Bahl–Cocke–Jelinek–Raviv (BCJR) algorithm [1], often provide good performance when operating in turbo equalizer setting. The complexity of the trellis-based equalizers, however, grows quickly in severe interference environments, especially when the interference occurs in more than one dimension.

There are a considerable body of work on the equalization of 2-D ISI that arises in recording channels, including feedback-based multitrack BCJR algorithm operating in row and column directions [2], the BCJR algorithm with data-dependent noise prediction [3], and suboptimal joint detection/decoding on Voronoi cells [4].

While it has been long known that linear equalizers (LEs) pay considerable noise enhancement penalty and thus do not perform well in high ISI environments, the work of [5] has shown that the SISO version of the LE performs surprisingly well in turbo setting; in 1-D ISI communication channels, the results of [5] reveal that for a wide range of ISI, the considerably simpler SISO-LE matches the performance of the optimum BCJR equalizer. This paper is a step toward investigating the potential of simple filter-based LEs in handling 2-D ISI. We specifically consider the self-iterating equalizer (SIE) based on multiple scans of 1-D component LEs used in conjunction with hard-decision side-track interference cancellation. Self-iteration (SI) refers to iterative exchange of soft information among simple, individually weak component equalizers [6]. For comparison, we also analyze the performance of the SIE replacing the component LEs with the 1-D BCJR equalizers. Comparison is also made against standalone 2-D equalizers based on linear filtering or BCJR algorithms defined on forced 2-D state masks.

Manuscript received March 20, 2015; accepted May 16, 2015. Date of publication May 22, 2015; date of current version October 22, 2015. Corresponding author: J. Moon (e-mail: jmoon@kaist.edu).

Color versions of one or more of the figures in this paper are available online at http://ieeexplore.ieee.org.

Digital Object Identifier 10.1109/TMAG.2015.2436994

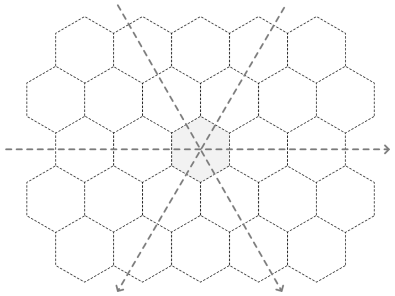

Fig. 1. 2-D array of hexagonal data cells and three equalizing directions.

Turbo equalization performance is conveniently analyzed using the EXIT chart [7]. In our SI setting, a component equalizer utilizes hard-decision feedback from a collaborating component equalizer, and it becomes necessary to modify the existing EXIT chart analysis method so that the mutual information (MI) transfer curves accurately reflect the quality of the hard decisions as well.

We shall compare the equalizers by investigating the required signal-to-noise ratios (SNRs) in opening up the tunnel in the EXIT chart. An opening between the MI transfer curves of the equalizer and the decoder in the EXIT chart indicates that repeated turbo iterations will eventually produce reliable decisions. The density thresholds beyond which no amount of SNR can allow reliable recovery of data for given equalizers are also investigated.

II. Channel Model

Consider a 2-D array of dense hexagonal storage cells, as shown in Fig. 1. Tightly deployed hexagonal cells allow highest packing density and for a given circularly symmetric read sensitivity function result in a severe from of multidirectional ISI. We assume that the write resolution is high enough to allow each cell to be fully magnetized independently of the neighboring cells so that the density limit is determined mainly by the effect of 2-D-ISI on signal processing. While more sophisticated write noise models exist that reflect pattern-dependence [3], [4], [8], here we assume that the noise is additive. While this signal and noise model appears highly simplified, we note that the equalization penalty is far greater

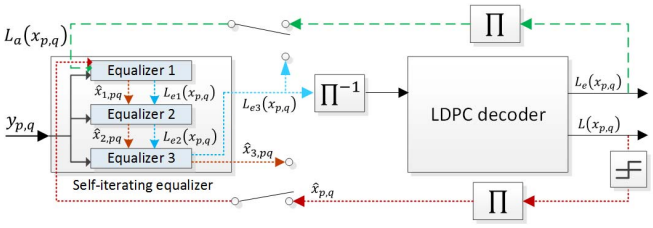

Fig. 2. SIE in turbo setting.

with additive noise than with write-pattern-dependent media noise. It is also true that the medium noise can be effectively countered using pattern-dependent noise prediction [9]. In these senses, our model can be viewed as a reasonable reflection of very severe ISI conditions.

Assume a 2-D Gaussian read sensitivity function [8] given as

$$h(i, j) = \exp\left\{\frac{-c(i^2 + j^2)}{2(T_{50}/T)^2}\right\} \tag{1}$$

where c is a constant, set to 1.8197; T_{50} is the half-height pulsewidth; T is the largest width of the bit cell; i and j point to the bit location in cross-track directon and down-track direction, respectively. Assuming that the front-end low-pass filter does not alter the head response noticeably, the discrete-time channel output can be written based on the sampled response of the read sensitivity function as

$$y_{p,q} = \sum_{(k,l)\in S_{p,q}} x_{k,l} h_{p-k,q-l} + n_{p,q} \tag{2}$$

where $x_{p,q} \in \{\pm 1\}$ represents the binary data, $S_{p,q}$ denotes a set of bits around the bit position (p, q), and $n_{p,q}$ is the zero-mean additive white Gaussian noise with variance σ_n^2. The SNR is defined as the total signal power captured in $y_{p,q}$ due to the bits in $S_{p,q}$ divided by σ_n^2.

III. Equalization Methods

A. Self-Iterating Soft Equalizer Based on 1-D Linear Component Equalizers

The equalizer of interest consists of multiple component 1-D LEs that generate soft decisions and exchange them with one another in the form of extrinsic information. In particular, each component equalizer is basically an LE running in one of three directions as shown in Fig. 1. Each component equalizer generates and passes the extrinsic information that becomes *a priori* symbol information for the next component equalizer. This process continues until decision quality no longer improves or enough overall iterations have been completed (Fig. 2).

The component equalizer takes the form of the soft linear minimum mean-squared error (MMSE) equalizer devised in [5]. Both the classical linear MMSE design and the SISO variation of [5] utilize the second-order statistics of the underlying noise and input bit sequences. The difference is that in classical design, only the *a priori* statistics of the input bit sequences could be utilized, whereas in the SISO version of [5], the equalizer design takes advantage of the input symbol statistics that effectively get updated in every turbo iteration by the way of improved soft decisions made available by the outer decoder. In our setting, the mean and variance of the bit decision values made available by the collaborating component equalizer, averaged over the entire block of bits, are used to reset the tap weights of the given component LE in the beginning of each iteration stage [6].

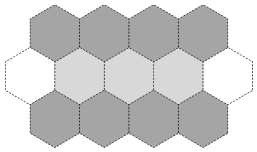

Fig. 3. Three cells aligned to the 1-D equalizer taps (gray cells) and eight side-track (dark gray) cells.

As the 1-D component LE slides along a given direction, there exist interferences coming from side tracks. This side-track interference is first canceled via hard-decision feedback ($\hat{x}_{j,pq}$ shown in Fig. 2) made available by the best up-to-date soft information in the collaborating component equalizer. Given the rotational symmetry of the hexagonal ISI pattern, the component equalizers running in other directions work in exactly the same way. Note that the passing of both the extrinsic information (shown as $L_{e,j}$ in Fig. 2) and the hard decisions occur in blocks, after each component equalizer completely scans the entire 2-D array of cells.

B. Improved Filter Coefficients Reflecting Hard-Decision Quality

Since the 1-D linear component equalizers utilize hard-decision feedback for side-track cancellation, the quality of the hard decisions may degrade the equalizer performance quickly under high ISI. To handle this issue, we develop a more effective 1-D component LE using enhanced filter coefficients (EFCs) that reflect the qualities of the hard decisions coming from the collaborating component equalizer.

The hard-decision feedback is determined by simple threshold detection of the updated log-likelihood ratio $L = L_a + L_e$ passed from the collaborating component equalizer. Each 1-D component LE in this paper uses three taps matched to the channel observations with the side-track interference subtracted out. Considering only the nearest interfering cells around a cell, there are eight side-track cells for each processing direction, as shown in Fig. 3. The variance of each side-track cell can be obtained using the updated soft information L as $v_{p,q}^o = 1 - |\bar{x}_{p,q}^o|^2$ where $\bar{x}_{p,q}^o = \tanh(L(x_{p,q})/2)$. For the first SI with zero L, the variances for offtrack cells are all set to 1. In order to retain the quasi-time-invariant (QTI) filter structure for minimum computational complexity, the time-averaged side-track variance $\bar{\bar{v}}^o = (1/M)\sum_{i=0}^{M-1} v_i^o$ (M is the data array size) is used to form the covariance matrix, i.e., $\bar{\bar{\mathbf{R}}}_{xx}^o = \text{diag}[\bar{\bar{v}}^o \cdots \bar{\bar{v}}^o]$.

Accordingly, the improved QTI taps are determined as

$$\mathbf{g}_{qti} = \left(\sigma_n^2 \mathbf{I}_N + \mathbf{H}^T \bar{\bar{\mathbf{R}}}_{xx} \mathbf{H} + \mathbf{H}_o^T \bar{\bar{\mathbf{R}}}_{xx}^o \mathbf{H}_o\right)^{-1} \mathbf{s} \tag{3}$$

where

$$\mathbf{H}_o^T = \begin{bmatrix} h_0 & h_1 & 0 & 0 & h_5 & h_6 & 0 & 0 \\ 0 & h_0 & h_1 & 0 & 0 & h_5 & h_6 & 0 \\ 0 & 0 & h_0 & h_1 & 0 & 0 & h_5 & h_6 \end{bmatrix}$$

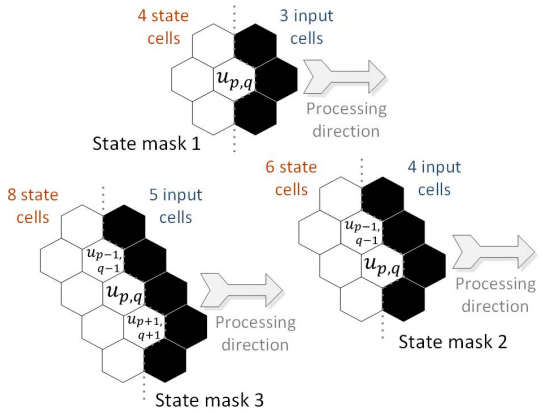

Fig. 4. State masks for the 2-D BCJR algorithm.

with h_i's representing the channel coefficients corresponding to the side-track cells for the given horizontal equalizing direction. The zeros are inserted to match the dimensions between $\bar{\bar{\mathbf{R}}}^{o}_{xx}$ and $\mathbf{H}^{T}_{o}$. The rest of the SIE process is identical to that described in [6] (or [10] for turbo setting).

C. 2-D Equalizers: BCJR and Linear

For comparison, we also describe a particular reduced-complexity BCJR algorithm running on a trellis diagram representation of 2-D ISI. The 2-D ISI in general cannot be decomposed into two 1-D ISI components (i.e., the D-transformation of the channel impulse response cannot be factored into two separate D-transformations) and thus does not lend itself to a finite-state machine description for complete ISI characterization. The consequence is that neither the maximum likelihood function nor the *a posteriori* probability can be computed in a recursive fashion with finite complexity.

The resort is often made to a suboptimal, reduced-state finite-state-machine description. While there are many choices when it comes to selecting a reduced-state machine, we force the family of state masks shown in Fig. 4. Three different sizes of the state masks are shown. The white cells correspond to the input symbols captured within a single state at a given time, while the black cells represent new input symbols. The state at a given time along with the given set of input symbols completely determine (assuming that ISI affects only the immediately neighboring cells) a set of noiseless channel outputs ($u_{p,q}$ for state mask 1; $u_{p-1,q-1}, u_{p,q}$ for state mask 2; and $u_{p-1,q-1}, u_{p,q}, u_{p+1,q+1}$ for state mask 3) that are used to compute the branch metric for the given processing interval. Note that it is possible to collect more noiseless channel output samples within the state mask utilizing decision feedback for the cells outside the mask, as has been done for 2-D rectangular ISI and state mask patterns in [2]. This will potentially improve the quality of the branch metric but also increases the complexity, and the resulting performance will depend highly on the specific feedback methods employed. Here, we opt to limit the number of observation samples used in branch metric computation as shown to make this reference system independent of the specific feedback technique employed. It is easy to see that the complexity depends exponentially on the number of white cells as well as the number of black cells.

The 2-D MMSE LE also used for comparison generates its soft decision based on a linear combination of the channel observation samples corresponding to the cells captured within a predetermined hexagonal filter mask [6]. The linear filter tap weights are computed basically following the method in [5] using the mean and average variance values of the updated input bit decisions by the soft outer decoder.

Note that while it is conceptually straightforward to use the 2-D BCJR or the 2-D MMSE equalizer as the component equalizers in our SIE set-up, doing so has little merit in our case, since rotating the state/filter mask along different directions makes little or no changes in terms of the specific interfering cells utilized to generate the nominal signal values for the branch metric calculation. We also note that unlike in [2], our 2-D BCJR schemes do not utilize feedback decisions, another reason why extra scans along additional directions do not collect significant independent information in our case.

IV. EXIT Chart Incorporating Hard-Decision Feedback

Turbo equalization performance can be analyzed using the EXIT chart that provides useful insights about iterative systems without time-consuming simulation of the full signal-processing chain [7]. The EXIT chart analysis is based on estimating the output of a component device in the form of extrinsic information L_e for a given value of the input *a priori* information L_a. However, in the SIE under investigation, a given component equalizer also utilizes the updated soft information L passed from the collaborating component equalizer (or the decoder in turbo setting) for side-track IC. To incorporate this feedback effect, we have devised a reasonable scheme to generate hard decisions using only L_a or, equivalently, L_e passed from the previous component equalizer (or decoder) [10]. These decisions are used to cancel the side-track interference during the simulation of the component equalizer for generating the histogram of its output or its extrinsic information that will be used for MI estimation.

First, we calculate MI $I(X;Y)$ using the histogram of an unequalized channel output Y and then extract the matching variance by $\epsilon_d = J^{-1}\{I(X;Y)\}$ via the function J of [7]. Then, the modeled $L = \epsilon_d x/2 + n(\epsilon_d)$ reflects decision quality available internally for all zero L_a, where $n(\epsilon_d)$ is Gaussian noise with zero mean and variance ϵ_d and $x \in \{\pm 1\}$ is the known data. Now assuming that the collaborating equalizer (or the decoder) provides *a priori* information, the decision improves to $L = \epsilon_t x/2 + n(\epsilon_t)$, where $\epsilon_t = \epsilon_d + \epsilon_a$ with a fixed ϵ_d and increasing ϵ_a. Finally, we get the required hard decisions from this L for the side-track IC. More detailed descriptions of the EXIT chart schemes for SIE can be found in [10].

V. Performance Comparison

The 2-D MMSE LE is based on a hexagonal 2-D filter mask FM3 that consists of 37 taps [6], whereas each 1-D component LE in SIE uses only three taps and the 1-D BCJR equalizer in SIE is formed on a four-state trellis with two branches for each state. The maximum number of SIs is fixed to 3 for the SIEs. The 2-D BCJR equalizers are based on state masks SM2 and SM3. The low-density parity check (LDPC) code employed is the array-based code of [11] with a codeword length of 8154 bits, a code rate of 0.907,

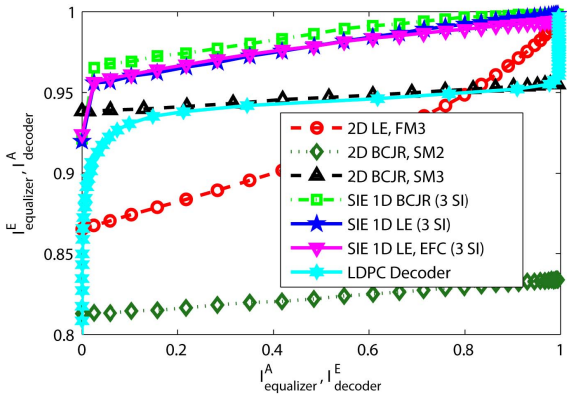

Fig. 5. EXIT chart for the different equalizers and the LDPC decoder: $T_{50}/T = 0.9$ and SNR = 13 dB.

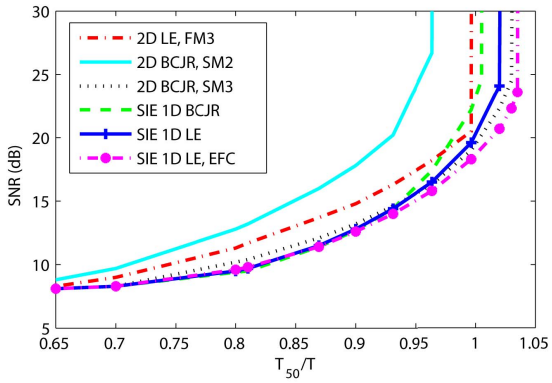

Fig. 6. Required SNR versus normalized density.

and a parity check matrix characterized by the column weight 5, the row weight 54, and the circulant matrix size of 139. The size of the 2-D bit array used in the simulation is 1024×1024 bits.

When assessing complexity in terms of the number of multiplications, the advantage of the 1-D LE-based SIE ($3N_L^2 MI$, where N_L is the 1-D filter length, M is the data array size, and I is the number of SI rounds) is considerable over the 2-D BCJR equalizer ($144KM \times 2^{3K}$, where K is the number of observations used for each branch metric computation). The 2-D MMSE equalizer complexity is given by $N_T^2 M$, where N_T is the number of taps in the 2-D filter mask and is also much higher than that of the SIE based on LE.

Fig. 5 shows that the SIE scheme based on 1-D LEs provides a much wider tunnel opening (in relation to the MI curve of the LDPC code) than the 2-D equalizers when the normalized density T_{50}/T is 0.9 and the channel SNR is 13 dB. In fact, under this channel condition, the three SIE methods based on 1-D component equalizers are the only schemes that allow the MI to reach the top-right corner of Fig. 5 (a full MI of one), indicating that they are the only schemes that will provide a reliable data recovery. Of the three, the 1-D BCJR-based SIE appears to give a very slight edge, and the use of the EFC does not seem to make difference under this channel condition. Although EXIT chart analysis is based on the idealized assumptions of infinite codeword length and Gaussianity of component device inputs, the bit error rate simulation results have been shown to be consistent with the analysis [6], [10].

Fig. 6 shows that the required SNR values for the three SIE schemes (which yield nearly identical curves) are smaller than the 2-D schemes at low densities. Up to the density near 0.94, all the three SIE schemes are better than the highly complex 2-D BCJR on SM3. For all practical densities, 1-D LE-based SIEs are better than 2-D MMSE on FM3, which is still more complex. The 2-D BCJR with SM2 is clearly the worst.

The upper limit on achievable density for a given equalization scheme is marked by the density where the required SNR shoots up quickly. The density limits for the 1-D linear SIE schemes and the highly complex 2-D BCJR with SM3 are very similar, reaching values between 1 and 1.05. The 1-D BCJR-based SIE has noticeable performance degradation relative to the 1-D LE-based SIE under very severe ISI. This is presumably due to the higher sensitivity of the BCJR scheme to mismatch between the extent of the actual ISI and the assumed mask size. When the EFC technique is employed, 1-D linear SIE even shows a density improvement, albeit small, over the considerably more complex 2-D BCJR with SM3.

VI. Conclusion

SIEs based on simple component equalizers are compared with 2-D equalizers that are more complex. The results indicate that for a wide range of 2-D ISI, the simple SIE made up of multiple 1-D LEs requires less SNR in opening an EXIT chart tunnel than more complex 2-D equalizers. The achievable density limit of the 1-D linear SIE has been extended using improved filter tap coefficients without increasing complexity.

Acknowledgment

This work was supported in part by the National Research Foundation of Korea under Grant 2010-0029205.

References

[1] L. Bahl, J. Cocke, F. Jelinek, and J. Raviv, "Optimal decoding of linear codes for minimizing symbol error rate (Corresp.)," *IEEE Trans. Inf. Theory*, vol. 20, no. 2, pp. 284–287, Mar. 1974.

[2] Y. Chen and S. G. Srinivasa, "Joint self-iterating equalization and detection for two-dimensional intersymbol-interference channels," *IEEE Trans. Commun.*, vol. 61, no. 8, pp. 3219–3230, Aug. 2013.

[3] B. Vasic *et al.*, "A study of TDMR signal-processing opportunities based on quasi-micromagnetic simulations," in *Proc. IEEE Magn. Rec. Conf. (TMRC)*, Berkeley, CA, USA, Aug. 2014, pp. 1–5.

[4] S. M. Khatami and B. Vasic, "Detection for two-dimensional magnetic recording systems," in *Proc. ICNC*, Jan. 2013, pp. 535–539.

[5] M. Tuchler, R. Koetter, and A. C. Singer, "Turbo equalization: Principles and new results," *IEEE Trans. Commun.*, vol. 50, no. 5, pp. 754–767, May 2002.

[6] J. No and J. Moon, "Multi-directional self-iterating soft equalization for 2D intersymbol interference," in *Proc. IEEE GLOBECOM*, Atlanta, GA, USA, Dec. 2013, pp. 2698–2704.

[7] S. ten Brink, "Designing iterative decoding schemes with the extrinsic information transfer chart," *AEÜ Int. J. Electron. Commun.*, vol. 54, no. 6, pp. 389–398, Nov. 2000.

[8] E. Hwang, R. Negi, and B. V. K. V. Kumar, "Signal processing for near 10 Tbit/in^2 density in two-dimensional magnetic recording (TDMR)," *IEEE Trans. Magn.*, vol. 46, no. 6, pp. 1813–1816, Jun. 2010.

[9] J. Moon and J. Park, "Pattern-dependent noise prediction in signal-dependent noise," *IEEE J. Sel. Areas Commun.*, vol. 19, no. 4, pp. 730–743, Apr. 2001.

[10] J. No and J. Moon, "Turbo equalization of 2D intersymbol interference using multiple 1D constituent equalizers," *IEEE Trans. Magn.*, to be published.

[11] E. Eleftheriou and S. Olcer, "Low-density parity-check codes for digital subscriber lines," in *Proc. IEEE ICC*, Apr. 2002, pp. 1752–1757.